Materials Research Proceedings 28 (2023) 667-674 https://doi.org/10.21741/9781644902479-72

Evolution of microstructure during hot incremental disk rolling of a nickel-based super-alloy

DINÇER Mehmet Şamil[1,2,a *], OZCATALBAS Mustafa[2,b], ACAR Sadik Sefa [1,2,c], MUSIC Omer[3,d] and ŞIMŞIR Caner[1,e]

[1]Middle East Technical University, Ankara 06800, Turkey

[2]Repkon Machine and Tool Industry and Trade Inc., Istanbul 34980, Turkey

[3]TED University, Ankara 06420, Turkey

[a]samil.dincer@metu.edu.tr, [b]mustafa.ozcatalbas@repkon.com.tr, [c]sadik.acar@metu.edu.tr, [d]omer.music@tedu.edu.tr, [e]csimsir@metu.edu.tr

Keywords: Hot Process, Recrystallization, FEM, JMAK

Abstract. In the aerospace industry, the turbine disk plays a crucial role. Controlling the average grain size during the hot forming of nickel-based superalloys such as Inconel 718 is critical for turbine disk production. Recrystallization is primarily responsible for evolution of microstructure during a hot forming process. In the current study, Finite Element Method (FEM) is employed to assess grain size evolution during an incremental disk rolling process. FEM simulations are used to obtain temperature, strain and strain rate distributions. Then, utilizing these deformation distributions, recrystallization and consequent average grain size distributions are calculated using Johnson-Mehl-Avrami-Kolmogorov (JMAK) equations. Simulations are conducted for different spindle rates of the workpiece. This process is sensitive to the temperature and meta-dynamic recrystallization. Results show that temperature increases with the spindle rate due to the inelastic heat generation. Also a higher grain size variation through thickness is obtained for the simulation with lower spindle rate since meta-dynamic recrystallization fraction is higher.

Introduction

A wide range of alloys have good mechanical properties at room temperature, however, only a few alloys can be used at elevated temperatures. The primary category of these alloys is Nickel-based superalloys. These properties are governed mostly by the microstructure [1]. The key to achieving good and uniform characteristics during the manufacturing process is being able to control the grain size. Most frequently used approach is to simulate the process using FEM. This provides an understanding of microstructure evolution of the material during the process and reduces the number of trials required for process development. The reason is that temperature, strain, and strain rate distributions are significant parameters affecting the grain size [2]. JMAK equations can calculate recrystallization fractions with these values [3].

At elevated temperatures, three different forms of recrystallization can occur. These are static, dynamic, and meta-dynamic [4]. Static recrystallization may occur if there is cold work in the material before heating. When the material is subjected to hot deformation, dynamic recrystallization takes place. A more accurate description of the occurrence of dynamic recrystallization is strain rate being greater than zero. Meta-Dynamic recrystallization is similar to static recrystallization, but it only occurs if the dynamic recrystallization fraction(X_{DRX}) is lower than 1 during the hot deformation process. Fig. 1 depicts the summary of the recrystallization phenomenon.

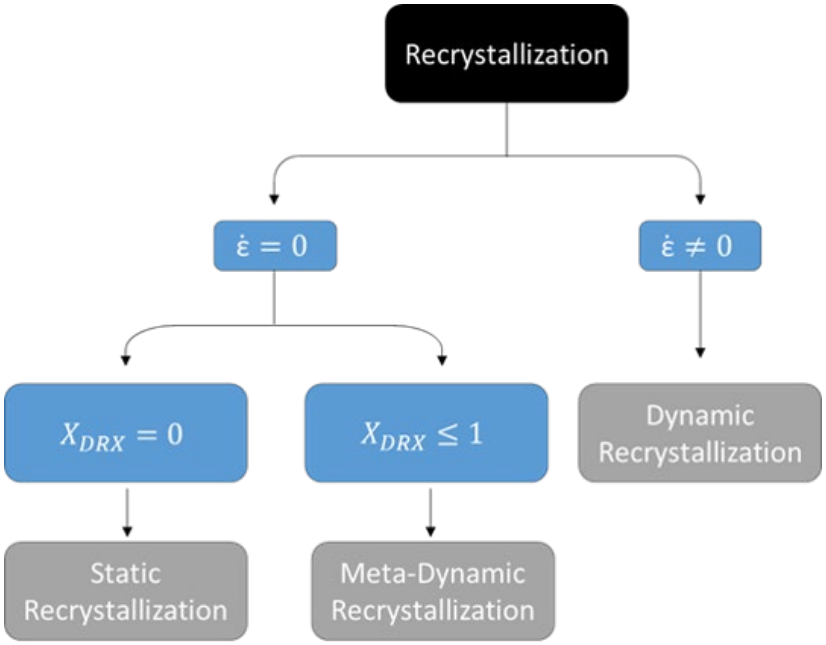

Fig. 1. Summary of Recrystallization.

All these calculations are covered by JMAK equations [3]. However, the majority of equations are empirical. Experiments have to be conducted to determine the material coefficients. To predict material parameters for recrystallization and grain growth, single and double compression tests have to be applied. Provided that the initial grain diameter is known, the single compression test is applied with different sets of constant strain rate and constant temperature. With these experimental results, dynamic recrystallization parameters can be obtained with the curve fitting method. To predict meta-dynamic recrystallization and grain growth parameters, a double compression test has to be applied with different combinations of strain rate, temperature, and waiting time between loadings [2]. These equations can be employed once the relationship between properties has been determined.

Dynamic recrystallization equations:

$$X_{DRX} = 1 - exp\left(A_1 \times \frac{\varepsilon(t) - A_3 \times {\varepsilon_c}^{A_2}}{\varepsilon_{0.5} - A_4 \times \varepsilon_c}\right) \quad (1)$$

$$\varepsilon_c = A_{crit} \times B_1 \times {d_0}^{B_2} \times \dot{\varepsilon}^{B_3} \times Z^{B_4} \times exp\left(\frac{Q_{B_5}}{R \times T}\right) \quad (2)$$

$$\varepsilon_{0.5} = C_1 \times {d_0}^{C_2} \times \dot{\varepsilon}^{C_3} \times Z^{C_4} \times exp\left(\frac{Q_{C_5}}{R \times T}\right) \quad (3)$$

$$D_{DRX\ Nuclei} = D_1 \times {d_0}^{D_2} \times \dot{\varepsilon}^{D_3} \times Z^{D_4} \times exp\left(\frac{Q_{D_5}}{R \times T}\right) \quad (4)$$

Meta-Dynamic recrystallization equation:

$$X_{MDRX} = 1 - exp\left(E_1 \times \left(\frac{t}{t_{0.5}}\right)^{E_2}\right) \quad (5)$$

$$t_{0.5} = F_1 \times \varepsilon^{F_2} \times {d_0}^{F_3} \times \dot{\varepsilon}^{F_4} \times Z^{F_5} \times exp\left(\frac{Q_{F_6}}{R \times T}\right) \quad (6)$$

$$D_{MDRX\ Nuclei} = G_1 \times {d_0}^{G_2} \times \dot{\varepsilon}^{G_3} \times Z^{G_4} \times exp\left(\frac{Q_{G_5}}{R \times T}\right) \quad (7)$$

Grain growth:

$${d_{grain\ growth}}^{H_1} = {d_0}^{H_2} + H_3 \times exp\ exp\left(\frac{Q}{R \times T}\right) \times t \quad (8)$$

Table 1. Parameters list.

Material coefficients	A_1-A_4	Dynamic recrystallization fraction
	B_1-B_5	Critical strain
	C_1-C_5	Half recrystallized volume fraction strain
	D_1-D_5	The average grain diameter of dynamically recrystallized fraction
	E_1-E_2	Meta-dynamic recrystallization fraction
	F_1-F_6	Half recrystallized volume fraction time
	G_1-G_5	The average grain diameter of meta-dynamic recrystallized fraction
	H_1-H_3	Grain growth
d_0		The initial average grain diameter
$\dot{\varepsilon}$		Strain rate
ε		Strain
Q		Activation Energy
R		Gas constant
T		Temperature
Z		Zener-Hollomon parameter
X_{DRX}		The fraction of dynamic recrystallization
$D_{DRX\ Nuclei}$		The average diameter of dynamic recrystallization
X_{MDRX}		The fraction of meta-dynamic recrystallization
$D_{MDRX\ Nuclei}$		The average diameter of meta-dynamic recrystallization
$d_{grain\ growth}$		The average grain diameter of grain growth

Recrystallization is governed by strain, strain rate, and temperature, as demonstrated by the preceding equations and Fig. 1. These equations are only applicable to isothermal conditions with a constant strain rate. However, the deformation in the hot incremental disk rolling process is not completely isothermal and the strain rate is not constant or uniform. Both strain rate and temperature are a function of time. To include that effect, these equations need to be updated with their differential form with respect to time [5]. However, assuming isothermal and constant strain rate condition is not a completely wrong assumption when the spindle rate is optimized accordingly as demonstrated in this study.

Modelling Approach

As the workpiece spins, four rollers deform the workpiece radially outward. As the thickness of the workpiece decreases, the outer diameter of the workpiece increases. Forge NxT commercial finite element software using implicit time integration scheme is used for the process simulations. These simulations consist of thermo-mechanical calculations. The Johnson-Cook plasticity material model is used to simulate the flow of bulk material in order to examine the history of temperature, strain, and strain rates. Ideally, process would be simulated as it is; however, this is not feasible due to large computational time. Instead, an angular segment of the disk is modelled

with boundary conditions applied at each side of the disk. These boundary conditions could be applied as cyclic symmetry boundary condition. However, this option is not available in the software at the moment. Instead, boundary conditions are applied as two planes which are adiabatic and allow for sliding of the nodes along the plane, but do not allow for node separation. Due to the numerical integration of the variables, the time step of the simulation has to be small for microstructure evaluation. To overcome this problem and reduce computational time, a comparison between angular segments of varying size and a full disk model was performed. This study showed that 1/8 angular segment of the disk produces similar results with full model. Results of the convergence study are not included here for brevity. As demonstrated in Fig. 2, the horizontal plane of the disk exhibits mirror symmetry. Thus, only top half of the disk can be used with symmetry boundary condition at the horizontal plane. The two boundary conditions applied through the planes do not fully reflect the nature of the process. Therefore, to minimize their effect on the results, only results for the middle of the angular segment are taken into consideration, as shown in Fig. 3 [6]. Rollers are assumed to be frictionless and do not rotate around their axes, the assumption being that the effect of friction can be neglected. Effect of friction and roller rotation will be examined separately in future studies. The temperature of the process atmosphere is controlled by a furnace. Heat transfer due to conduction between the rolles and the workpiece, radiation and convection with the environment are all included together. Value taken is: 50W/m^{2}K which is the average of the value widely available in the literature. The metallurgical part of the calculations is uncoupled with a thermo-mechanic solver. Outputs of the thermo-mechanical model are used to calculate the recrystallization and growth mechanism. Mechanical and thermal parameters of Inconel 718 are taken from JMatPro material property simulation software and the JMAK equations parameters are taken from Forge NxT Software.

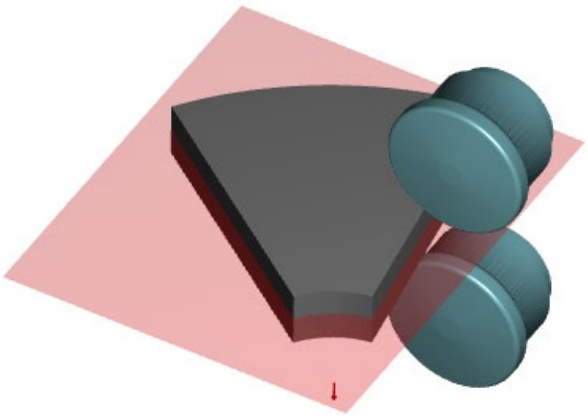

Fig. 2. The simulation model of an incremental disk rolling.

Results and Discussion

This section simulates and compares the effect of three distinct spindle rates (RPM of the workpiece). Fig. 3 illustrates the portion of the simulated part that is shown in the subsequent figures.

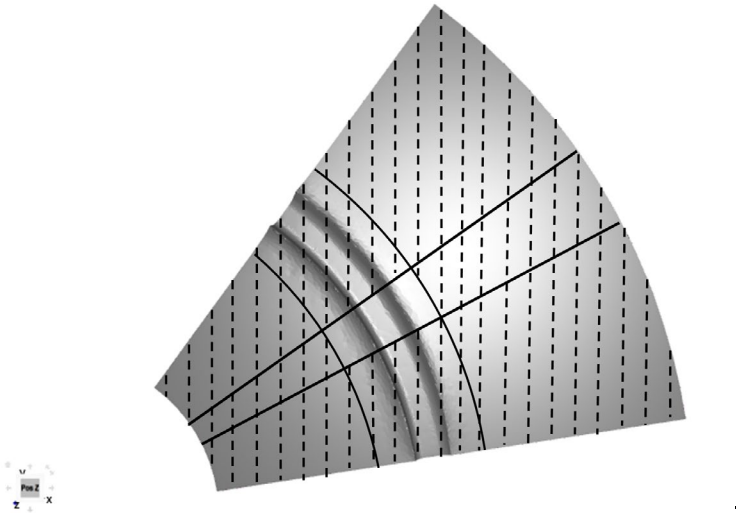

Fig. 3. Comparable area of the simulation model.

The results of simulations with three different spindle rates are evaluated. Temperature, equivalent strain, dynamic recrystallization, meta-dynamic crystallization, and average ASTM grain diameter are compared. The spindle rate has a significant effect on the temperature. The inelastic heat generation increases as the deformation rate increases. Temperature change is not found to be important unless it exceeds the range of the JMAK equation parameter. Despite grain growth being unaffected at the time scale of the first pass, it will be modified during the rest of the process. The other issue is that the temperature exceeds 1030°C for the fastest spindle rate case, as seen in Fig. 4(c). This temperature level is close to the upper limit of the JMAK equation parameter range for Inconel 718. These limits come from the processing map of Inconel 718. 1030°C is the most efficient temperature for the dynamic recrystallization range for forged Inconel 718 [7]. It was shown that the material starts to behave differently above this temperature [3]. The equivalent strain is also strongly affected by the spindle rate as it is an expected result due to the nature of the rolling process as shown the Fig. 5. Results show that equivalent strain values are very high even after the first pass for the high spindle rate case. The reason for having different equivalent strain values for the same thickness reduction is that the plastic flow in the circumferential direction increases when the spindle rate is increased. For high spindle rates, elements become elongated not only in the radial direction but also in the circumferential direction.

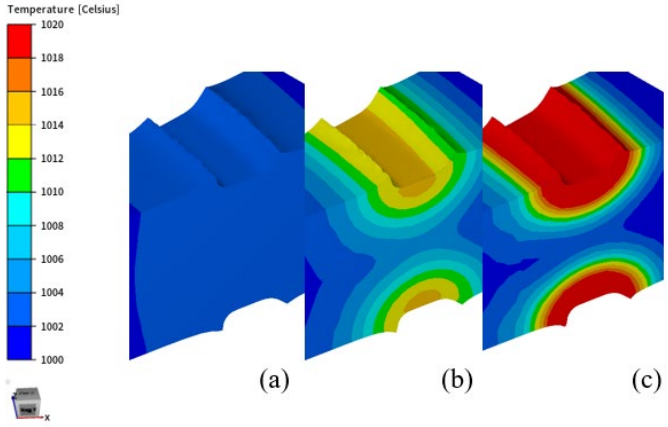

Fig. 4. (a) The lowest spindle rate, (b) medium spindle rate, (c) fastest spindle rate result of temperature distribution during the process.

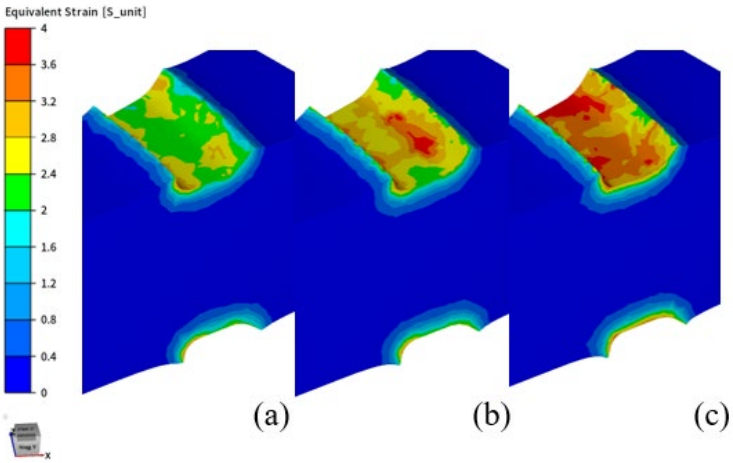

Fig. 5. (a) The lowest spindle rate, (b) medium spindle rate, (c) fastest spindle rate result of Equivalent strain distribution during the process.

Dynamic recrystallization occurs due to the deformation. Temperature, strain, and strain rate change over time. Therefore every parameter in Eq. 1 is affected even though the dynamic recrystallization equation contains no time parameter. The area of dynamic recrystallization fraction is almost constant throughout the first pass for different temperature and equivalent strain values, as shown in Fig. 6. When the deformation rate increase with the spindle rate, the critical strain (ε_c) value and half recrystallization fraction strain ($\varepsilon_{0.5}$) value increase. So the affected dynamic recrystallization zone stays the same.

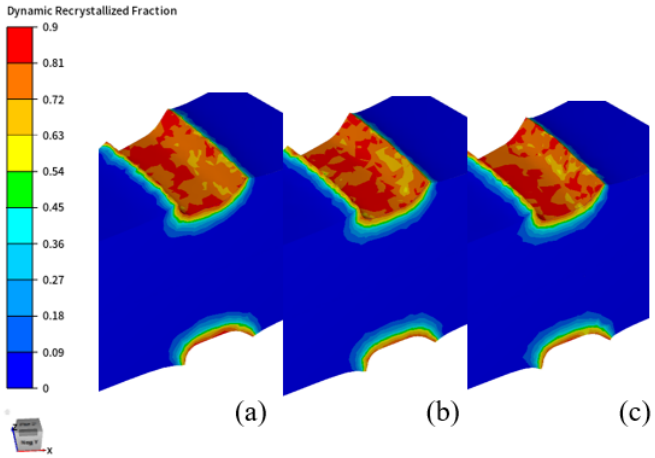

Fig. 6. (a) The lowest spindle rate, (b) medium spindle rate, (c) fastest spindle rate result of dynamic recrystallization distribution during the process.

The area of meta-dynamic recrystallization is affected by the spindle rate since changing the spindle rate modifies the time interval between two subsequent passes. The primary variable in meta-dynamic recrystallization is the time. When the spindle rate is low, meta-dynamic recrystallization can take place over a longer period of time, as shown in Fig. 7.

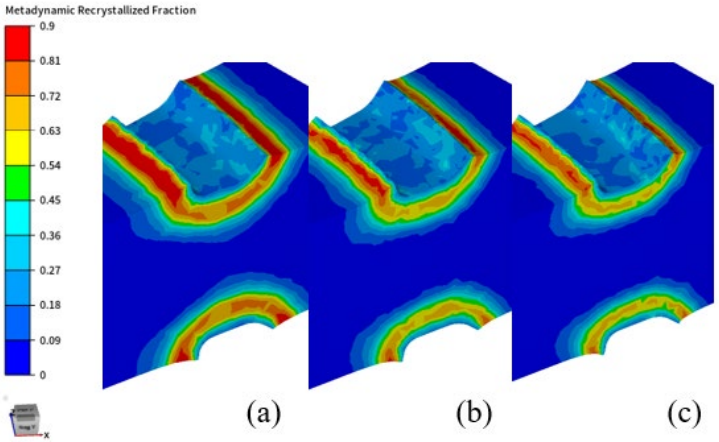

Fig. 7. (a) The lowest spindle rate, (b) medium spindle rate, (c) fastest spindle rate result of meta-dynamic recrystallization distribution during the process.

Fig. 8 illustrates the variation of the average grain diameter with the spindle rate. Recrystallization plays a substantial role in grain size reduction. Although the overall recrystallization zone is similar in all three simulations, the time between subsequent passes is high for low spindle rate. Therefore lower spindle rate leads to a higher variation of ASTM grain size through the thickness due to the meta-dynamic recrystallization.

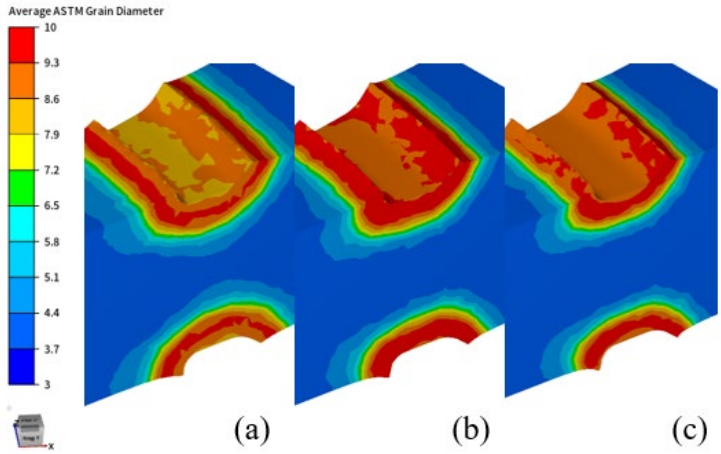

Fig. 8. (a) The lowest spindle rate, (b) medium spindle rate, (c) fastest spindle rate result of average ASTM grain diameter distribution during the process.

Summary

These results demonstrate the significance of the spindle rate as a process parameter in hot incremental disk rolling. The temperature increases dramatically at high spindle rates due to inelastic heat generation. The stability of the JMAK equations depends on the temperature. At the slowest spindle rate, temperature change is negligible. When the spindle rate increases, elongation in the circumferential direction becomes considerable. Effects of equivalent strain and temperature cannot be observed in the first circumferential pass for dynamic recrystallization. On the other hand, the area of meta-dynamic recrystallization is influenced by the spindle rate. The time between subsequent passes decreases when the spindle rate is increased. Therefore, the meta-dynamic recrystallization fraction decreases as the spindle rate increases. Forming with a lower spindle rate leads to a higher variation of ASTM grain size through the thickness. There was no linear dependence found between average ASTM grain size and spindle rate. The optimum spindle

rate is between the lowest and the medium spindle rate. The limiting factors of spindle rate range are temperature change which is important for JMAK equation stability and meta-dynamic recrystallization fraction which changes the variation ASTM grain size through the thickness.

Acknowledgment
This work was supported by The Scientific and Technological Research Council of Türkiye, TÜBİTAK.

References
[1] C.T. Sims, A history of superalloy metallurgy for Superalloy Metallurgists, Superalloys 1984 (Fifth International Symposium), 1984, 399-419. https://doi.org/10.7449/1984/Superalloys_1984
[2] G. Shen, S.L. Semiatin, R. Shivpuri, Modeling microstructural development during the forging of waspaloy, Metall. Mater. Trans. A 26 (1995) 1795–1803. https://doi.org/10.1007/bf02670767
[3] S.H. Mousavi Anijdan, M. Aghaie-Khafri, V. Joshaghani, Forging optimization and microstructural simulation of an Inconel 718 alloy used in turbine discs, J. Appl. Math. Phys. 05 (2017) 1658-1667. https://doi.org/10.4236/jamp.2017.59138
[4] C.M. Sellars, J.A. Whiteman, Recrystallization and grain growth in hot rolling, Metal Sci. 13 (1979) 187-194. https://doi.org/10.1179/msc.1979.13.3-4.187
[5] T. Matsui, H. Takizawa, H. Kikuchi, Numerical simulation of ring rolling process for ni-base articles, Superalloys 2004 (Tenth International Symposium), 2004. https://doi.org/10.7449/2004/Superalloys_2004_907_915
[6] O. Music, E.C. Sariyarlioglu, Mechanics of Tube Spinning: A Review, Int. J. Adv. Manuf. Technol. 123 (2022) 709-735. https://doi.org/10.1007/s00170-022-10175-6
[7] Y.V.R.K. Prasad, S. Sasidhara, K.P. Rao, Hot working guide: A compendium of processing maps. Materials Park, OH: ASM International, 1997.